ROYAL INSTITUTE
OF TECHNOLOGY

Microwave assisted synthesis of thermoelectric nanostructures: p- and n-type $Bi_{2-x}Sb_xTe_3$

VIKING ROOSMARK

Master of Science Thesis

Department of Applied Physics

KTH – Royal Institute of Technology

Stockholm, Sweden 2018

Supervisor

Mr. Bejan Hamawandi

bejan@kth.se

Examiner

Prof. Muhammet S. Toprak

toprak@kth.se

Biomedical and X-Ray Physics

KTH/Albanova

SE-106 91 Stockholm

TRITA-SCI-GRU 2018:416

Abstract

Improving the way energy can be obtained, is becoming increasingly important from both environmental and economical aspects. Thermoelectric (TE) materials can be a stepping stone in the right direction for better energy management, seeing how they can recycle waste heat and generate electricity from energy that otherwise would be wasted. In recent years TE materials have been the focus of several projects to find materials which can easily and inexpensively be used in devices to harvest heat and produce clean energy, which is aimed by this project. TE nanomaterials based on the $Bi_{2-x}Sb_xTe_3$ system with different stoichiometry (x) have been synthesized using a bottom-up microwave (MW) assisted synthesis method. Nanopowders have been consolidated with SPS into pellets to examine their TE transport properties. The purpose of the project was to fabricate p- and n-type TE materials with comparable thermal expansion, for the purpose of obtaining a high efficiency TE device with high durability. The MW assisted synthesis shows highly reproducible results with nanopowders having good uniformity with low to none batch to batch variation in the powder composition. One of the most important aspects of this technique is the process speed, the MW heating itself only takes 2-3 min to synthesize the desired TE material using the developed thermolysis route. In comparison to some other bottom-up methods, which takes multiple hours -up to several days, the MW-assisted synthesis have a very high energy and time efficiency. Transport evaluation showed a smooth transition from n- type to p-type by increasing Sb concentration -where $x > 0.5$. The highest TE figure-of-merit, ZT, value of 1.04 was obtained for n-type and 0.4 for p-type synthesized materials at 448 K. These results are comparable to state-of the art values for n- and p-type bulk Bi-Te materials, showing the feasibility of the developed method and materials -for their use in energy harvesting TE devices.

Sammanfattning

Att förbättra tillvägagångssättet som energi produceras, har blivit viktigare och viktigare från både ett ekonomiskt och miljöperspektiv. Termoelektriska (TE) material kan komma att bli ett steg i rätt riktning för hur energihantering fungerar. Då dessa material kan återvinna spillvärme och producera elektricitet från energi som annars skulle slösas. Under de senaste åren så har TE material varit i fokus för flera projekt som syftat att hitta material som både enkelt och billigt kan användas i ändamål för produktion av ren energi från spill värme, vilket även är målet för detta projekt. TE nanomaterial baserade på $Bi_{2-x}Sb_xTe_3$ familjen med olika stökiometri (x), har syntetiserats genom en botten-upp mikrovågs (MV) syntetiserings metod. Nanopulver har konsoliderats med SPS till pellets, för att sedan undersökas och få sina TE transport egenskaper analyserade. Projektets mål var att tillverka p- och n-typ TE material med liknande termiska expansioner, med syftet att använda dessa i en hög effektiv TE anordning med hög uthållighet. Den valda MV metoden visar högt reproducerbara resultat med nanopulver som har bra uniformitet och låg variation i komposition mellan olika kullar. En av de viktigaste aspekterna för denna teknik är processhastighet, uppvärmningen pågår endast 2-3 minuter för att syntetisera TE materialet. Som jämförelse tar vissa andra botten-upp metoder flera timmar eller dagar, vilket gör att MV metoden i jämförelse blir väldigt energi och tids effektivt. En utvärdering av transport data visade en smidig övergång från n-typ till p-typ när Sb koncentrationen var $x > 0.5$. Det högsta värdet för TE värdesiffran ZT, blev 1.04 för n-typ och 0.4 för p-typ och erhölls vid 448 K. Dessa värden är jämförbara med state-of the art värden för både n och p-typ Bi-Te material, vilket visar möjligheterna för den använda metoden och de resulterande materialen att komma att användas i rollen som energi återvinnande TE enheter.

Table of contents

1. Background

The purpose of nanotechnology is to study or manipulate materials with a size limitation below 100 nm and is an area with a wide range of possible applications. From food products to space and satellite development, to medicine and electronics nanotech can be applied to several vastly different fields of research. As technology pushes to become smaller, more compact and at the same time perform with higher efficiency, one has to examine new ways of manufacturing and producing these materials and devices, as well as developing new fabrication methods. One of the bases of nanotechnology is to increase efficiency per area/volume ratio unit, which can be used for either improving performance or reducing the device size or ideally improving both characteristics at the same time. So it's easy to see why many industries would be interested in nanotech in one way or another as the application area is very broad and is not fixed on one single way of enhancing the end product. Products can be improved upon in other ways, such as giving them entirely new functionality e.g. self-cleaning cloths or solar panels that can work both as a power source and a window[1, 2].

Many researchers and companies are now looking for ways to utilize nanotech for improving or inventing products in their respective fields. One of the most common areas of interest is the energy sector, were batteries, vehicles, solar energy and other renewable energy sources are of interest. A relatively new source of renewable energy are thermoelectric materials and their ability to recycle waste heat into electricity. These materials and devices as well as different ways of improving upon their material properties and performance, is the main focus of this work.

1.1 Thermoelectricity

Thermoelectric (TE) materials and devices have in recent years been the subject of an increasing amount of interest from researchers and studies for the purpose of energy recycling and as a power source for electronics[3]. The special property of TE materials is their ability to convert a difference in temperature across a material, directly into electricity and vice versa, this is an example of the TE effect. The explanation for these materials being able to convert heat into electricity, is the fact that a heat difference in matter will cause unbalanced potential in the two ends of a TE material, to correct this unbalance the majority carriers moves from one side to the other and creates a current flow.

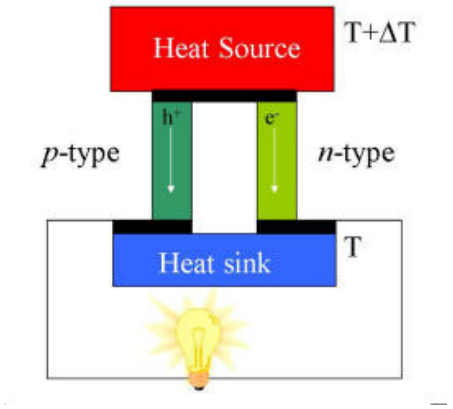

Figure 1. Schematic showing how a TE device works[4].

The performance of a TE device is dependent on many factors. The dimensionless figure of merit ZT is an indication of the TE performance of the material. $ZT = \sigma S^2 T/\kappa$, where σ is the electrical conductivity, S is the Seebeck coefficient defined as the induced voltage from a temperature difference, T is the absolute temperature and κ is the thermal conductivity. All these factors affect how well a material performs as a TE device[5].

1.2 Synthesis methods

There are important factors which need to be taken into consideration when synthesizing TE materials. Such as the synthesis method and the chemical route used for making the material. There are several manufacturing techniques to fabricate TE materials, they can mainly be summarized into two groups. The first one is the chemical solution route which is best described as classic chemistry where solvents and liquids are used. Some techniques included in this group are solvothermal, chemical vapor deposition and electro chemical deposition methods, all of these are examples of a bottom up synthesis. The other family of synthesis methods are the physical techniques, they commonly use force and temperature for producing the material. Methods included here are grinding, ball milling, melting and other forms of mechanical alloying, which is summarized as top down synthesis.

A very promising solvothermal chemical synthesis method is the microwave (MW) assisted synthesis method, which have been used for synthesis of TE materials in earlier works[6, 7]. This method for producing TE materials have many important advantages, the most significant is the short time synthesis, which only takes minutes[8–12]. Compare this to some of the other solution chemical techniques which can go up towards days, one can see that this advantage can nearly not be overstated. Other strong sides are the homogeneous heating of the solution, the end result will be a more homogenous product and reproducible with high yield. The power efficiency and environmental aspects of the methods are also worth taking into consideration. A major factor which plays a huge role in any large-scale production is the reduction and elimination of human errors making the whole process more reproducible, even this is an aspect

improved with MW synthesis, as a number of steps are automated by the microwave machine. So there are many reasons why MW synthesis can be a strong contender for industrial scale manufacturing of TE materials, the most important one is the heating mechanism that may selectively activate the precursors used.

1.3 Bulk nanomaterial consolidation with SPS

There is the subject of consolidating the powders obtained from synthesis into compact solid pellets. This is most commonly done by placing high pressure and temperature on the powder to compress it into pellets, one example of this process is Spark Plasma Sintering (SPS).The pressure and temperature influences the nanostructure, by inducing grain growth on the particles[13, 14]. SPS does have many advantages when compared to normal sintering, such as higher density and often smaller micro structures which is needed for improving the TE transport properties and in turn means that these compaction method can improve the TE performance[15–18]. Though the SPS method is good from a density standpoint it is worth looking into other forms of consolidation methods for the TE powders if preserving the nanostructure is of great importance, as SPS changes the nanostructure. If an approach that doesn't change the structure could be used there is a great potential for the ZT value to be vastly improved.

1.4 Bismuth chalcogenide system

There is a great interest in the $Bi_{2-x}Sb_xTe_3$ system, for room temperature TE applications both as an n-type material and a p-type material, as this system can be both. Pure Bi_2Te_3 is one of the most commonly used and researched n-type TE materials, while $Bi_{0.5}Sb_{1.5}Te_3$ has become a widely known p-type material with good TE performance. Some have suggested these materials to be the highest performing of their system for their respective type[12, 19, 20]. The Bi_2Te_3 system have been the subject of many studies, and synthesizing techniques both top down and bottom up e.g. electro deposition[21]. This work will focus on MW synthesis as one of the bottom up methods, some work have been done previously studying bismuth telluride synthesized by MW-assisted synthesis [8, 11, 12].

When synthesizing Bi_2Te_3 one should start by putting Te into containers and then the Te powder is mixed with Trioctylphosphine (TOP), followed by MW-assisted heating. $BiCl_3$ is mixed with 1,5-Pentanediol and Thioglycolic acid (TGA), this solution is then mixed with the Te-TOP solution to synthesize the TE powder. In this work a new variation of this procedure has been used, the main differences are the replacing of TOP with Tributylphosphine (TBP) and 1,5-Pentanediol with ethylene glycol (EG). The purpose of the work is to develop a new highly-efficient and scalable process for synthesizing TE materials and examining and finding the optimal parameters for the new method. It's also of interest to observe if there are any changes of the TE properties and how the ZT changes.

There could be significant improvements made to TE devices by making a device with n-type and p-type materials of similar compositions as these devises would not have any problem with asymmetrical thermal expansion during the operation of the device. The obvious requirement that is needed for a device of this kind to be useful is a high TE performance (ZT) in both materials. Therefore, there is an interest in finding two compositions of the $Bi_{2-x}Sb_xTe_3$ system that both have relatively high ZT, one being n-type the other being p-type and for these two compositions to be similar to one another. For this purpose, it is of utmost importance to properly determine the composition in this system where the p-n transition lies, which is the place where the majority carrier changes from electrons to holes and wise versa. There has been a great amount of articles debating which the composition is, where the p-n transition takes place. The span of potential compositions is quite wide and no real consensus have been reached as of today. Indeed, there seems to be a big number of different factors one has to take into consideration for finding the composition where n- to p- transition takes place.

1.5 Compositions with p - n transition

For the purpose of improving TE devices there are many aspects which have to be taken into consideration, not only the ZT, power factor and other material properties, but one also have to mind the device design. Otherwise one can risk having a device with well performing base materials, which still can at the end be low performing. As mentioned earlier an asymmetrical thermal expansion coefficient can ruin a working good device, if the aim is to make better performing TE devices with p and n materials from the same systems it would be wise to consider the compositions and if possible using compositions close to the p-n transition. For the $Bi_{2-x}Sb_xTe_3$ system compositions ranging from x = 0.5 and 0.4[8, 22] to 1.88[23] have been suggested to be where the p-n transition takes place. Those are the extremes though and most articles suggest it to be somewhere between x being 1.0[24–27] or 1.2[28] to 1.4[29]. Some factors which seem to play a big role for the p-n transition are temperature, size of the device, extrinsic doping and possibly structure and synthesis. The thickness of the samples e.g. if they are thin films, as compared to nanoplates and pellets can play a role, or if the samples are polycrystalline or single crystal could mater. Furthermore it seems like a rise in temperature can make n-type materials change into p-type, with and excess amount of Te one can turn p-type into n-type if the composition is $x \leq 0.5$, if $x > 0.6$ a donor is needed for the same effect[25]. Most sources seem to agree that the optimal composition for p-type is around $x = 1.5$[8, 12, 19, 20, 29] and pure Bi_2Te_3 is the most efficient n-type[19].

There are plenty of articles mentioning their n-p transition compositions in the $Bi_{2-x}Sb_xTe_3$ system. These compositions can vary vastly depending on the methods used and for different groups and the parameters of the obtained samples. As such, a need to go through many different reference articles and methods used, to be able to decide which compositions to synthesize, and which composition have the highest ZT.

Many groups have used physical methods such as melting, grinding and powder metallurgy to make Bi-Sb-Te based TE materials, there are a number of works which have used these methods and discussed the p-n transition. Different compositions around $Bi_{0.5}Sb_{1.5}Te_3$ were processed by powder metallurgy methods (such as grinding, pressing melting) and then examined to study the TE figure of merit for the different composition and particle size[20]. The BiSbTe system was studied and the transport properties of Bi_2Te_3 and Sb_2Te_3 are presented. A phase diagram was used to help identifying which compositions result in n-type materials. These samples were made with mechanical alloying and ball milling[26]. Bismuth antimony telluride samples were synthesized by melting and mechanical alloying. The samples were studied to determine the composition, and to study the impact the compositions and different anneal temperatures have on the TE performance [28]. Polycrystalline and single crystal $Bi_{2-x}Sb_xTe_3$ are both examined and compared for their TE performance as the point of interest. These samples were prepared with different methods such as mechanical alloying, melting and grinding. It was found that the polycrystalline samples contrary to the single crystal samples have a p-n transition when the Sb percentage is increased[29]. By changing the ratio of Bi and Sb in $Bi_xSb_{2-x}Te_3$ by melting and cooling, one can change the bulk carrier density and even the carrier type[24].

Solution based techniques in general and MW-assisted techniques in particular are of interest for this work, seeing how MW-assisted synthesis is the method chosen and used. This means that articles using MW-assisted synthesis and discus their transition composition are of great importance. One such group used microwave assisted synthesis of Bi_2Te_3 and Sb_2Te_3 nanoplates. The nanoplates were then mixed and BiSbTe pellets were made and examined for their TE transport properties[8]. Other groups have discussed the ZT and ways to improve it with graphene. MW-assisted synthesis of p-type $Bi_{0.5}Sb_{1.5}Te_3$ with added extended graphene was examined to determine the impact of the graphene on the TE properties of the material. It was found that the addition of the extended graphene improved the ZT value with 45% compared to samples without graphene[12].

There were many other methods used but the amount of literature was less, and these are methods which won't be used for this work, but never the less it's still important to examine their results.

One method which was used to synthesize $Bi_{2-x}Sb_xTe_3$ and also discussed the majority carrier transition was ECD. In this work nanowires of p-type $Bi_{2-x}Sb_xTe_3$ were deposited with pulsed laser assisted ECD, an improved Seebeck and electrical conductivity was achieved compared to their normal results. Higher TE performance achieved compared with materials fabricated with other methods[19].

Chemical vapor deposition (CVD) is a method which can be used to synthesize bismuth telluride, it can also achieve low dimensions on the obtained structures. Thin nanoplates (9-42nm) of $Bi_{2-x}Sb_xTe_3$ have been synthesized with CVD and have a composition range of x = 0.14-1.9. The highest TE figure of merit was reached at $x = 1$ and it was also found that an

increasing amount of Sb lead to stronger p-type behavior with $x = 0.5$ as the composition where the material goes from n-type to p-type[22]. With the help of molecular beam epitaxy $Bi_{2-x}Sb_xTe_3$ was grown and the band structure of the compositions could be tuned. The purpose of the work was to examine and design topological insulators. The obtained p-n transition point in this work was decided to be $Bi_{0.12}Sb_{1.88}Te_3$[23]. Samples obtained through Bridgman growth were examined and TE properties were found. The carrier properties are of great interest and so is the band gap. Specifically the thermal band gap were determined through calculations and data from the analysis of the samples[25]. P-type nanoplates of bismuth antimony telluride were synthesized with a solvothermal method. The composition and carrier concentration are tuned to find the highest figure of merit, which were obtained at $Bi_{0.5}Sb_{1.5}Te_3$ and had a value of 0.51[27].

Table 1. Survey of p-n transition composition from different methods and sources.

Composition	Structure	Thickness	Synthesis	Characterization methods	Ref
$Bi_{1.5}Sb_{0.5}Te_3$	NP	16 nm	CVD	EDS,TEM, 4 Probe	[22]
$Bi_{0.12}Sb_{1.88}Te_3$	Film layers	5nm	MBE	ARPES,RHEED,ICP-AES	[23]
$Bi_1Sb_1Te_3$	NP, SC	5-10 nm	VSG	ARPES,TEM, EDX	[24]
$Bi_{0.8}Sb_{1.2}Te_3$	PC, Pellets	12 mm	Mechanical	Microprobe, Thermo couples	[28]
$Bi_{0.6}Sb_{1.4}Te_3$	PC, Pellets	5 mm	Mechanical	XRD	[29]
$Bi_1Sb_1Te_3$	SC, Ingots	80 mm L 10 mm D	Bridgman Growth	Micro-thermoprobe Line Scans	[25]
$Bi_1Sb_1Te_3$	PC, Cylinder	15 mm L 20 mm D	Mechanical	XRD,Electron microprobe, SEM	[26]
$Bi_{1.6}Sb_{0.4}Te_3$	NP, Pellets	2-5 mm	MW	XPS,XRD,SEM, TEM, Electron microprobe	[8]

PC:Polycrystalline; **SC**:Single Crystal; **NP**: Nanoplates

From the literature there were many different compositions suggested for the n-p transition composition, with varying synthesis methods. When choosing which compositions to synthesize for the p and n materials, the commonly used $Bi_{0.5}Sb_{1.5}Te_3$ for p type and the highest performing n type material from another MW-assisted synthesis work[8] which is $Bi_{1.8}Sb_{0.3}Te_3$ were chosen. With these materials the goal is to make a device with high ZT and even thermal expansion. Calculations were made to decide the proper amounts of precursors necessary for the wanted compositions and for it to be stoichiometry correct for 1 g of precipitated powder. The chosen compositions along the fraction of each element in each composition can be seen in the Appendix table 1, with the molecular weight of each TE element needed for 1 gram of the desired powder in the Appendix table 2 and the amount of precursors in weight can be seen in the Appendix table 3. The calculations were made by calculating the molar mass of each composition which depends on the molar mass and amount of each TE element in them. From

the molar mass of the compositions, the fraction and weight in grams for each element can be decided and the last step is calculating the required amount of precursors needed for the synthesis. The amount of precursors can be obtained by knowing the molar mass of all the precursors in combination with the previously calculated weight of each TE element. From the weight of elements, the proper amount of moles of each element in each composition is obtained and from the element moles, the moles of precursors needed is calculated. With the precursor moles and molar mass know, it's simple to get the weight of all the precursors.

1.6 Objectives

The purpose of this work can be summarized to a couple of points of interest. Using a new synthesis process based on MW assisted heating, evaluate the reproducibility of the process and the quality of the resulting powders. It is also aimed at synthesizing both n- and p- type TE material from the same materials family to be used for TE device fabrication later on. Sb content in the powder composition will be tuned as the key factor for n- to p- transition. Lastly the TE results will be investigated and compared to the literature, to evaluate if the TE materials have comparative ZT value to the state-of-the art.

2. Experimental procedure

2.1 Synthesis

Multiple batches of $Bi_{2-x}Sb_xTe_3$ material were synthesized for determining the optimal parameter of the synthesis processes. Parameters such as the duration of the heating, and which order the chemicals were mixed. The general outline of the process is described in the following diagram, fig. 2, $Bi_{2-x}Sb_xTe_3$ was synthesized with an altered technique from previous literature [8, 9, 11, 12].

All the precursors and elements were stoichiometrically weighted and calculated for as to be as precise as possible for the synthesis of the $Bi_{2-x}Sb_xTe_3$ composition. The $BiCl_3$, $SbCl_3$ and Te powder were all of reagent grade 98% or above and obtained from Sigma-Aldrich. As a general guideline one should always take care when weighing, measuring or in any way handle chemicals in a lab, all the reactions and measurements were performed in a fume hood for safety reasons. To weigh the precursors it's best to do it gradually and slowly by putting small amounts multiple times in containers. In this work 20 mL microwave vials were used, this way it will be harder to accidentally put in too much material in any steep and possibly ruin a delicate reaction, as one can always add more material to the container, but rarely remove it.

The process is started by measuring 0.478-0.611 g Te powder, depending on the composition being made and putting it into the microwave vials with a volume of 20 mL, then TBP (3 mL) is added to the Te powder via a syringe. This solution is then mixed with spinning magnets that are placed in the vials beforehand over a hotplate for a time interval of 10-30 sec and then ultrasonicated for 15 min to break up any remaining powder aggregates. The solution is then put in a microwave for heating, the heating lasts for 90 secs at 220 °C after this process a yellow Te-TBP solution has been obtained observed in fig. 3.

$BiCl_3$ and $SbCl_3$ were both mixed with EG (10 mL). The mixing was done first with the help of spinning magnets for a minimum of 30 min and then ultrasonication for 15 min for further mixing. The next step was to mix this solution with TGA (0.5 mL) to gain a thioligated pnictogen solution and is followed by further mixing by ultrasonication for 15 min. The Te-TBP solution is then added to the thioligated pnictogen solution via syringes with the resulting mixture seen in fig. 4, this mixture is then placed in a microwave. The heating process is initiated with pre-steering for 2 min and then heated at 220 °C for 2 min and will result in a dark gray solution fig. 5.

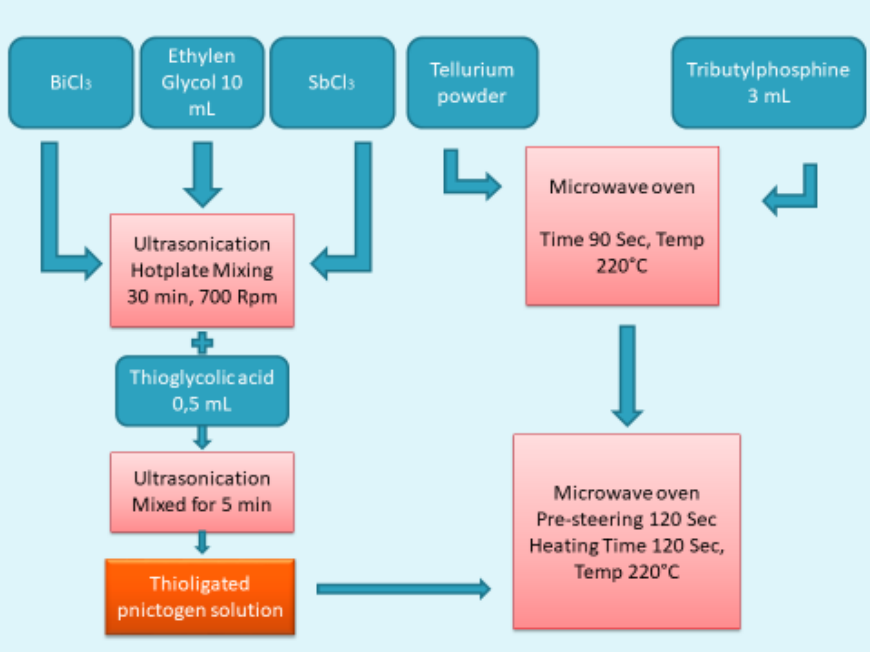

Figure 2. Synthesis diagram of the TE powders.

After a short time period of cooling down the precipitated powder will sediment as seen in fig. 6 and is expected to weigh around 1 g. The powder is then separated from the solution with centrifugation, filtering and washing with isopropanol and acetone for removal of EG and other unwanted particles. The filtering and washing is done in four steps, first pour out the majority of the EG out of vials. The second step is to pour isopropanol into the vials and to mix the isopropanol with the remaining EG and powder, the vials are then shaken by hand and by machine for thorough mixing. The vials are centrifuged for 3 min with a speed of 8000 RPM which is followed by separating the isopropanol from the sediment powder by pouring the isopropanol out of the vials. Acetone and lastly isopropanol are respectively used in the same manner as step two for step three and four out of the cleaning process. The last step of the process is drying the samples in a furnace for removing any remaining solvents. Magnets were put into the Te-TBP and thioligated pnictogen solutions for better mixing.

The first batch made was aimed to yield 7 g worth of $Bi_{0.5}Sb_{1.5}Te_3$ powders. It was made to follow the general synthesis process with the exception that the TBP and Te powders were prepared in two bigger vials with 2.28 g Te powders and 12 mL TBP in each vial. The final microwave heating was set to last for 2 min for this batch.

The second batch had an expected yield of 2 g $Bi_{0.5}Sb_{1.5}Te_3$ with the major difference between the first and second batch being the distribution of the Te-TBP solution with less concentration. In this case 0.57 g of Te powder was mixed with 3 mL TBP, and this was done to examine any possible difference between the two different procedures. The yield in the way of obtained weight of powder for each sample was around 85-90% of the theoretical maximum.

The last four batches were all made with the intention of yielding 8 g worth of their respective compositions, and then to be used for making pellets through SPS. These pellets will then be used in thermoelectric characterizations to obtain the thermoelectric properties inherent to their respective powders. When synthesizing the four last batches the standard synthesis process were followed, as this method was the easiest and yielded the purest grade powders of all the processes.

For the purpose of optimizing the process from a time perspective, batches of Bi_2Te_3 with twice the amount of the required chemicals as compared to the regular batches were tried. The only exception was EG which was reduced to 6 mL from 10 mL so that the vials have the right amount of liquid for the MW heating process to work. The advantages with this new process would be a time reduction close to half the time needed and also less total materials needed for the synthesis of the materials. Also during this updated method another step of ultrasonication was added for the Te-TBP solution, with the aim to improve the mixing of the Te and TBP which in turn would lead to better mixing with the thioligated pnictogen solution. It could be observed that there was no leftover Te powders in the Te-TBP solutions when ultrasonication was used, which has been the chase for batches without this added step.

A high amount of pressure arises during this process which can impact the results from the synthesis, this can to some extent be counteracted by adjusting the microwave oven to handle high adsorption liquid mediums which uses a slower heating process. With the pressure solved, we found a new technique to obtain twice the amount of material per batch with a reduction of 75% of EG used, however an extra peak was observed in the XRD pattern.

For the synthesis of the pellets the single method was used as the method with twice the material produced for each batch was deemed to unreliable to be used at the current time. As there were a chance for high pressure and inconsistencies in the trial of this method as well as an extra peak in the XRD pattern for this method. The next step is the examination of the powders with SEM and XRD to determine the micro-nanostructure, composition and searching for potential impurities. The last steep of the process is the compression of the synthesized powders to compact pellets, this was done with a SPS (SPS-825 system). Powders of 6-8 grams is preferable when making pellets to make sure that there is enough material for a full pellet, this was done for each of the four compositions of interest.

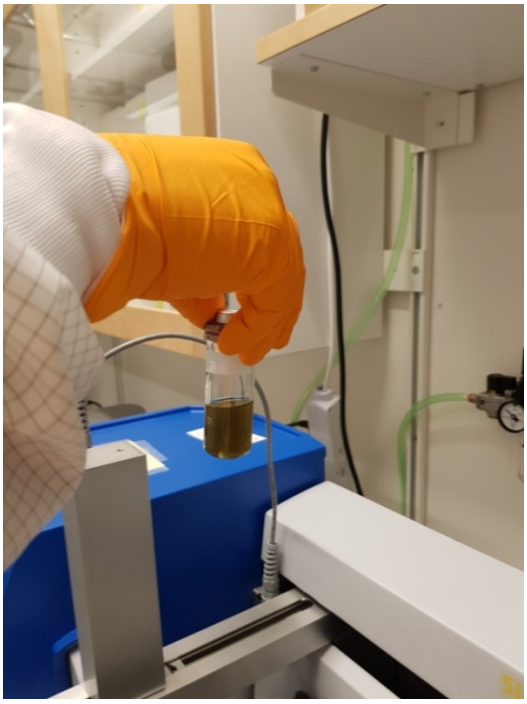

Figure 3. Te-TBP solution after microwave heating

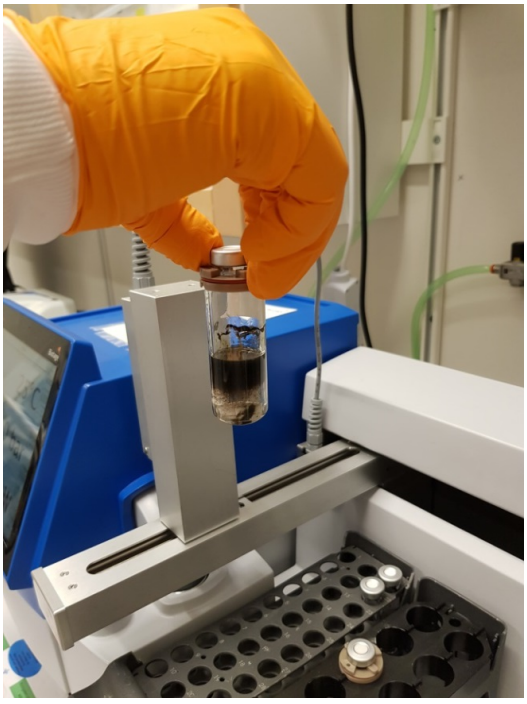

Figure 4. Thioligated pnictogen solution mixed with Te-TBP

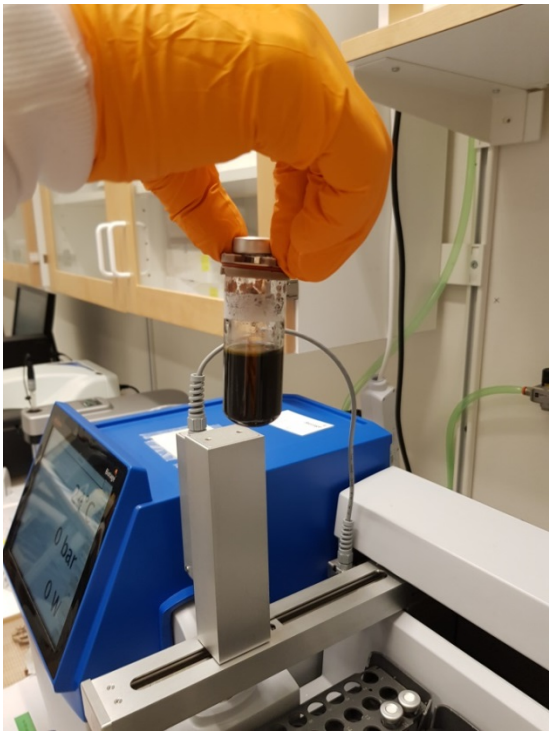

Figure 5. Sample from Fig 4 after microwave heating

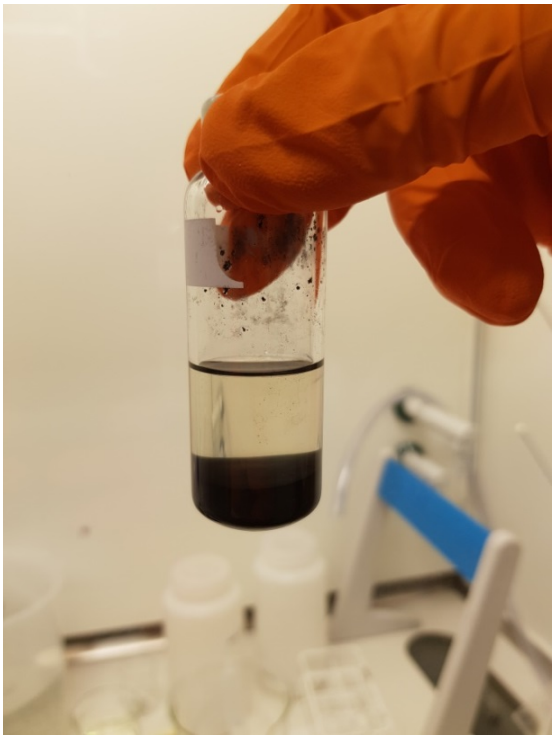

Figure 6. The powder has separated from the liquid

2.2 The BiSbTe phase

The crystal structure and microstructure of the samples were determined with X-ray powder diffraction and SEM (FEI Nova 200) respectively. The material phases of the $Bi_{2-x}Sb_xTe_3$ system was determined by using Rietveld refinement through a software program MATCH!

2.3 SPS Sintering

All powders were processed with the same parameter for the SPS method. This was done so the transport properties of the pellets would be comparable. The chosen temperature was set to 400 °C, with a heating rate of 50 °C /min. Pressure during SPS is crucial and helps deciding the density of the final pellets, for this project a load of 75 MPa was chosen. The holding time was set to 1 minute. Finally, the pellet have to be cooled, this process last for 15 min and the temperature went from 400 °C to 250 °C, at the same time the load decreased from 75 to 0 MPa. The pellets are now ready to be removed from the die for further analysis.

2.4 Transport properties

For the purpose of obtaining the figure of merit ZT from the synthesized samples one need to collect data on the TE properties of fabricated samples. The processes for doing this was developed in a previous project[30]. The Seebeck coefficient $\boldsymbol{S}$ and the electrical conductivity $\boldsymbol{\sigma}$, could both be measured at the same time with an ULVAC-RIKO ZEM3 system. To calculate the total thermal conductivity $\boldsymbol{\kappa}$ one has to first know the specific heat capacity $\boldsymbol{C}_p$, thermal diffusivity D and density ρ, then the equation $\kappa = C_p * D * \rho$ can be solved. The density of the samples could be obtained from Archimedes method, a laser flash analysis system (LFA 457, Netzsch) was used for obtaining the thermal diffusivity. A differential scanning calorimetry (Netzsch-DSC 404 Pegasus214 Polyma) was used to measure the specific heat capacity C_p. The thermal range used during the tests ranged from 298 K to 623 K, and with all the properties know the TE figure of merit ZT can be calculated.

3. Results & Discussion

3.1 SEM Analyses

SEM images fig. 7-9 were captured of samples from all batches of powders to examine the micro-nanostructures. The images were also used to confirm if the processes gives similar structures between batches, or in other words if the results are reproducible. Also there are certain TE properties which are greatly affected by different structures in materials, the nanostructure nature of the material improves the TE properties as an example. For the purpose of achieving higher figure of merit ZT one have a hand full of properties which can be focused on. Such as Seebeck coefficient, electrical and thermal conductivity, often the electrical and thermal conductivity have a strong relationship which can be a problem for TE materials, seeing how one wants the lowest possible thermal conductivity at the same time as the highest possible electrical conductivity. One way of achieving lower thermal conductivity is by having a nanostructure with as many grain boundaries as possible. The reason for this is the higher impact the boundaries have on phonon transport, in other words the thermal transport, than the transportation of electrons which is the electrical conductivity. With different types of doping the electrical conductivity can be increased, as the increased number of charge carriers will naturally increase the electrons transported across the material.

From the first batch type, fig. 8 (a)-(d) one can observe a majority of smaller hexagonal plates with approximate sizes of 0.1-0.6 μm on average in their largest dimensions, these are bismuth antimony telluride particles. These plates have for the most part a homogeneous size and similar shape. There are also some larger elongated particles which are suspected to be tellurium ranging from 3-5 μm on their widest dimension. These particles are most likely residue tellurium from the synthesis who haven't reacted fully, or there was a small excessive amount of tellurium in the synthesis process. This can be more or less confirmed by the XRD results from the same samples, which show some small traces of tellurium in otherwise mostly $Bi_{0.5}Sb_{1.5}Te_3$.

The second batch type, fig. 9 (a)-(d) and fig. 7 showed similar hexagonal nanoplates with sizes approximately ranging from below 80 nm up to 400nm and none of the tellurium particles. There are some few larger hexagonal plates which most likely are a result of some particles starting their grain growth earlier than others during microwave heating. The particles which have grown larger ranged on average from 1 to 3 μm. The second batch was tested separately for both samples included in the batch, and they both showed similar structures and gave identical XRD patterns, the method can therefore be deemed to be reproducible and yielding good quality materials.

The double material batches was found to have a small amount of excess tellurium which could be observed in SEM, but was undetected by XRD analysis. This can be explained by the Te content being lower than 5% of the whole material composition and would in that case be hard to detect with XRD analysis. There is a possibility that the Te will transform during SPS and

result in samples with no excess tellurium. In any case the fact that the double material batches cause problems in either the MW synthesis or not getting the intended composition, is a serious flaw and should therefore be avoided until a more stable method of doing this process is found.

There is no clear reason for the majority particles from both the first batch and the second batch to vary. If even the variation is relatively small, both batches have particles in the same span, but the first batch have more particles in the upper limit of that span than what the second batch have. This could be a small batch to batch variation, or it could be caused by the excess tellurium.

In fig. 10, 11 powders from $Bi_{1.8}Sb_{0.2}Te_3$ and Bi_2Te_3 are shown respectively. Both these batches were made with the standard process and ended up with similar particles to that of $Bi_{0.5}Sb_{1.5}Te_3$ both in shape and size. The hexagonal structure of these particles stem from their crystal structure, which belongs to the hexagonal crystal family.

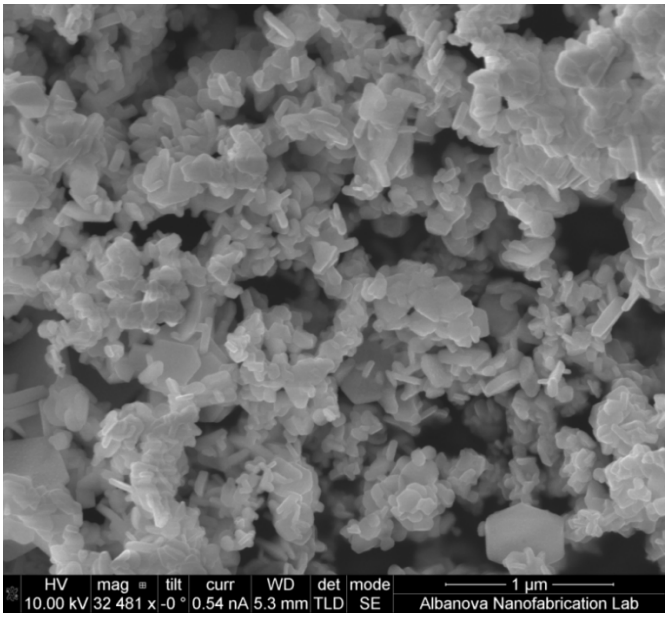

Figure 7. SEM image of the second $Bi_{0.5}Sb_{1.5}Te_3$ batch.

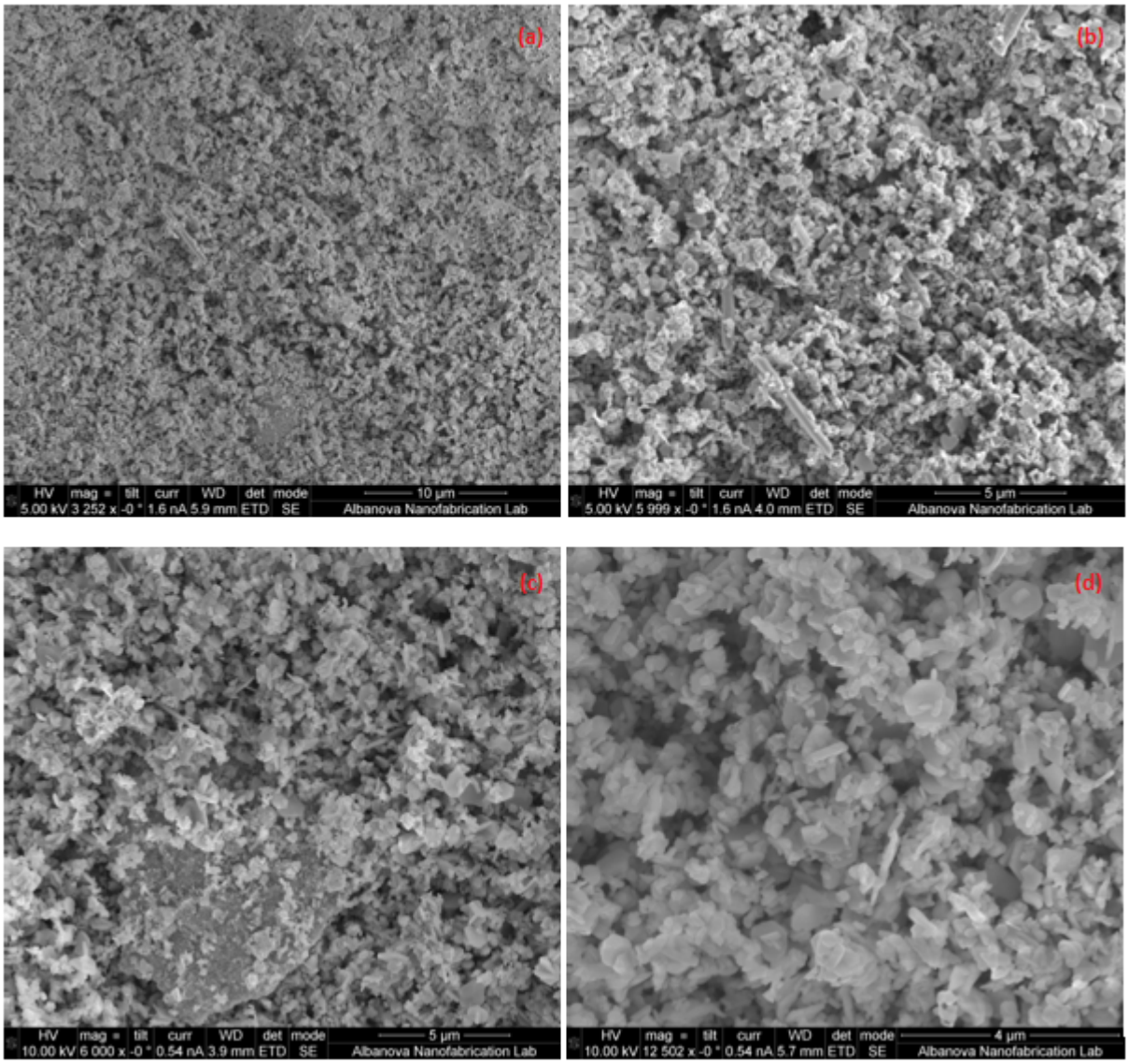

Figure 8. SEM images of the first $Bi_{0.5}Sb_{1.5}Te_3$ batch, (a) Gives a large overview of the particles, (b) is a zoomed in location from (a) which gives a more detailed view, the supposed Te particles are more easily spotted here. (c) Shows many micro particles in combination with a larger micro particle, (d) is a zoom in of (c) to better show the plate form of the particles

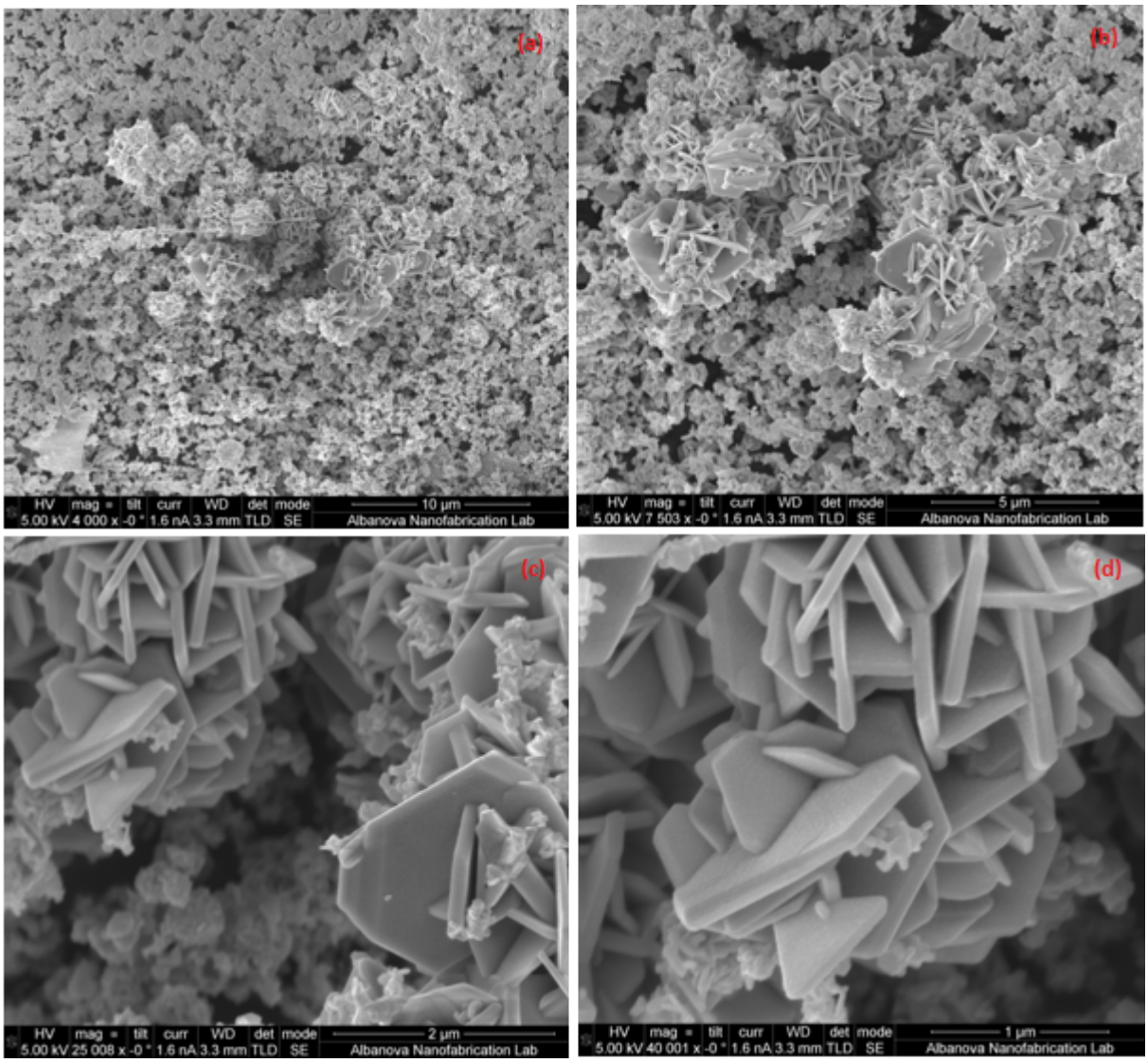

Figure 9. SEM images of the second $Bi_{0.5}Sb_{1.5}Te_3$ batch, (a) An overview of the particles, (b) is a zoomed in location from (a) which give a more detailed view, were many micro particles can be observed as well as some macro particles. (c) Is a further zoomed in picture of (b), and shows the hexagonal plate nature of these particles, (d) shows how these particles can intersect right through each other.

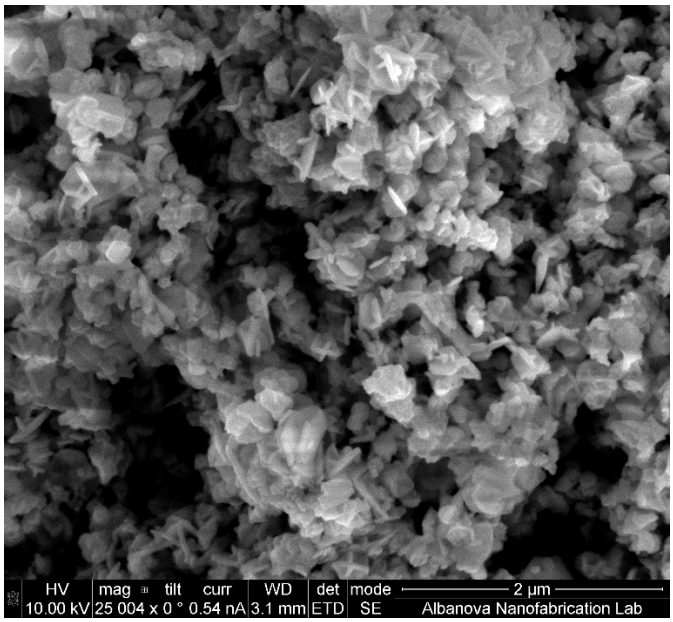

Figure 10. SEM image of $Bi_{1.8}Sb_{0.2}Te_3$ powder produced with the developed MW-assisted process.

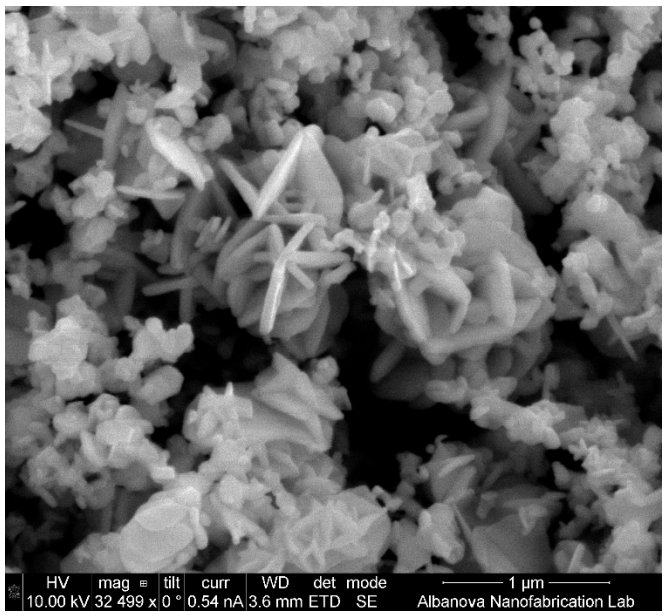

Figure 11. SEM image of Bi_2Te_3 powder produced with the developed MW-assisted process.

3.2 XRD Analyses

All powders and pellets produced have been analyzed with XRD and therefore x-ray powder diffraction patterns have been obtained for all our samples and can be seen in fig. 12 and 13. What can easily be observed from these plots, specifically fig. 12, is the shift of the peaks for all the samples. This shift follows a trend of going from the left to the right side with higher

amounts of antimony in the respective samples. If one remembers Bragg's law and the following conditions of $n\lambda = 2d\sin\theta$, where λ is the incident wavelength, most commonly this will be the Cu wavelength of 1.54 Å, d is the spacing between crystal planes and θ is the scattering angle of the x-rays, n is just an integer number. When taking this equation into account, one can calculate the distance between crystal planes in each XRD plot. As the λ is constant and the θ is given by dividing the x axis from the XRD plots by two, the only remaining variable is the spacing d. With increasing θ the interplanar spacing will decrease, which is easily understood from Bragg's law, $n\lambda / (2d\sin\theta) = 2d$. When d has been obtained one can also obtain the lattice constant a, for the crystal unit cell, one can use the following equation.

$$d = \frac{a}{\sqrt{h^2 + k^2 + l^2}}$$

Where the h, k, and l are the miller indices of the Bragg plane, from these formulas it can be calculated that peaks in the XRD plots with higher θ results in a lower lattice constant a. So it is noted that with higher amounts of antimony in the samples the lattice constant will shrink. This can be explained by antimony having smaller lattice constants than bismuth, which on happenstance is completely true. Antimony has a lattice constant of 4.262 Å while bismuth has 4.395 Å, which means that the shift of peaks in the produced samples makes sense.

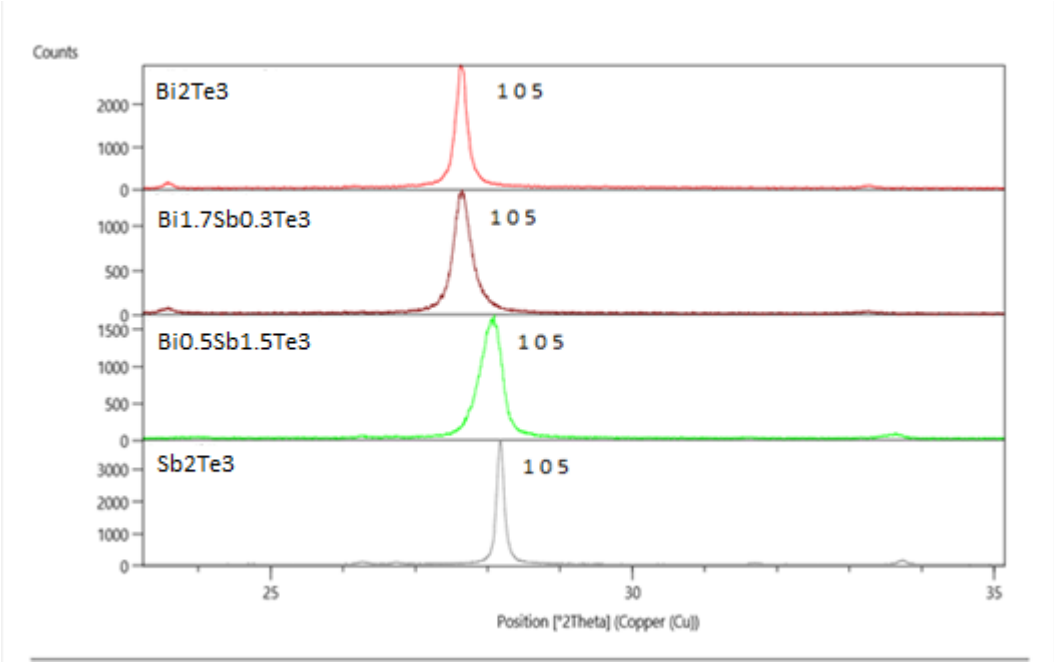

Figure 12. XRD powder patterns from the first synthesis trials, focusing the peak with miller indices of 105.

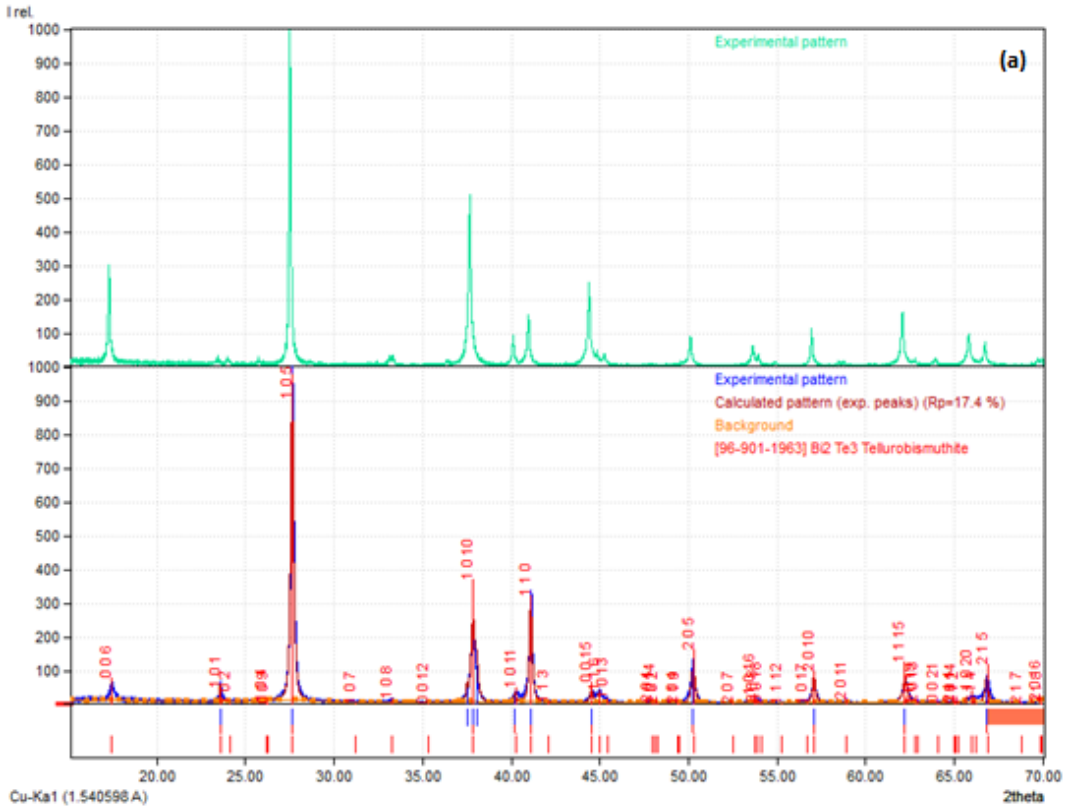
I rel.
Experimental pattern
(a)
Experimental pattern
Calculated pattern (exp. peaks) (Rp=17.4 %)
Background
[96-901-1963] Bi2 Te3 Tellurobismuthite
Cu-Ka1 (1.540598 A)
2theta

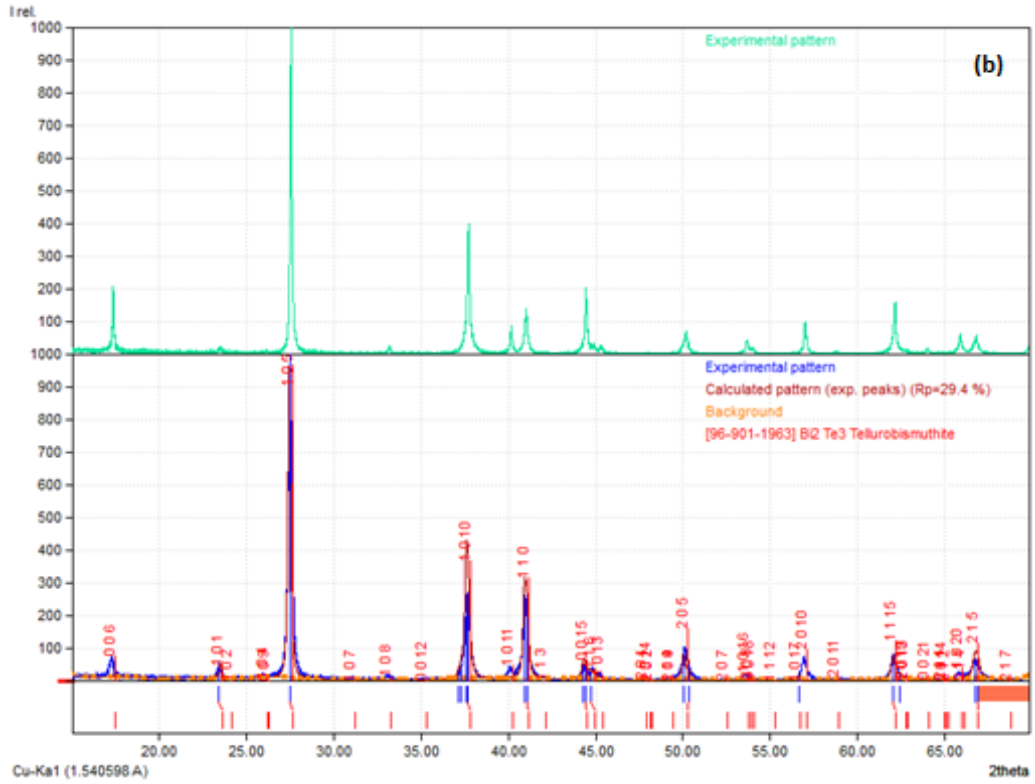
I rel.
Experimental pattern
(b)
Experimental pattern
Calculated pattern (exp. peaks) (Rp=29.4 %)
Background
[96-901-1963] Bi2 Te3 Tellurobismuthite
Cu-Ka1 (1.540598 A)
2theta

Figure 13. XRD analysis of synthesized $Bi_{2-x}Sb_xTe_3$ samples, (a)-(d) XRD patterns of $Bi_{2-x}Sb_xTe_3$ before and after SPS compression, (a) Bi_2Te_3, (b) $Bi_{1.8}Sb_{0.2}Te_3$, (c) $Bi_{0.5}Sb_{1.5}Te_3$ and (d) Sb_2Te_3.

It can clearly be observed that the SPS have affected the composition of the pellets from what they had in powder form. The XRD plots from fig. 13 (a)-(d) for each pellet is different from what they had as powders. What is interesting to note is the change in their match with the respective XRD database values and how the changes are vary for the different samples. The better matching powders of Bi_2Te_3 and Sb_2Te_3 both had score matches around 90%, however they score lower as pellets in the XRD database. But on the other hand $Bi_{1.8}Sb_{0.2}Te_3$ didn't get the exact match but something close and $Bi_{0.5}Sb_{1.5}Te_3$ had very good match with the new database values as powders, but as pellets the compositions got better match results. This could be due to residual Te and precursors which had not reacted and when put under high amounts of pressure and temperature they either transformed or evaporated. This is more likely for the compositions that mix Sb and Bi, as there are more reactants involved and harder to balance the tellurium reactions in those experiments. But in the case for the decreasing matches, it might be harder to explain, but the most likely explanation is the high temperature and pressure affect the crystallographic structures of the samples. Therefore, changes in the XRD spectra of these pellets are expected as the material has a coarse effect as they got packed in smaller volume.

3.3 Transport Property Evaluation

TE transport properties were obtained and studied from the pellets, made from TE nano-powders. The specific heat capacity $\boldsymbol{C}_p$ could not be obtained from the samples (because of some technical problems) and therefore values had to be obtained from the literature. The $\boldsymbol{C}_p$ for Bi_2Te_3, Sb_2Te_3 and $Bi_{0.5}Sb_{1.5}Te_3$ were taken from Ref. [31–34] and the $\boldsymbol{C}_p$ of $Bi_{1.8}Sb_{0.2}Te_3$ were calculated from the other specific heat values. By combining the experimentally obtained properties and the obtained $\boldsymbol{C}_p$ values the TE figure of merit ZT could be calculated and plotted for each sample at different temperatures, fig (14) (e). The top ZT value of 1.04 occurred at 448 K for the Bi_2Te_3 pellet. What is interesting to note about the high points of ZT for each pellet is the fact that all pellets except Sb_2Te_3 have increasing ZT values as the temperature rises, on the other hand Sb_2Te_3 have a drastically decreasing ZT profile for increased temperature. The value of 1.04 is on comparable levels as some of the previous works that have synthesized Bismuth telluride [8, 35], with values over or at 1.0 being reported.

The Seebeck coefficient from fig. 14 (c) indicates that the pellets with antimony have a positive doping and the pellets with bismuth have negative doping. As was expected both from sources in the literature and the fact that Bi and Sb act as negative and positive doping respectively. It can also be observed that there is a gradient, were the samples with mixed compositions are less positive/negative than what their parent composition are. The optimal condition would be two compositions who both are approximate to the zero Seebeck coefficient line to eliminate as much asymmetrical expansion as possible and yet have high values of ZT.

It should also be noted that the density value for each composition was lower than the theoretical densities. This is in a way common, as one rarely gets 100% of any theoretical value, but in this case the densities are a bit lower than one would typically expect, with densities of 80 to 90% of the theoretical values. The reason for diverging from the theoretical values and indeed for some of the samples densities to have higher accuracy than others are the amount of air trapped in the samples and the porosity. One of the more believable reasons for this could be the effects from the SPS method, as observed earlier, the SPS did affect the XRD patterns of the produced pellets, and would therefore have a high possibility of affecting the samples' crystal structures.

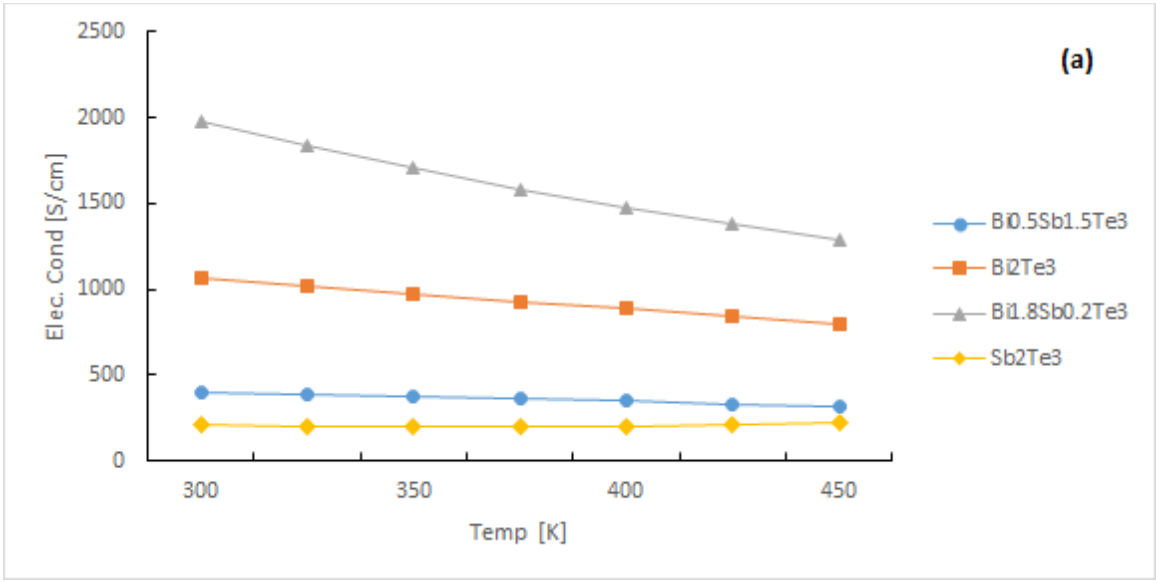

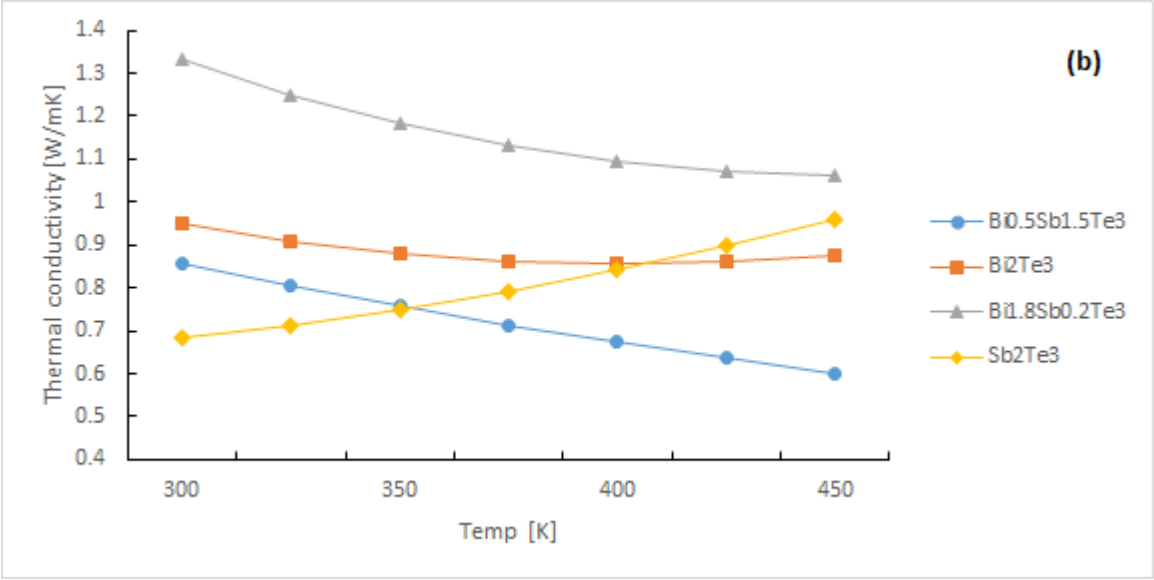

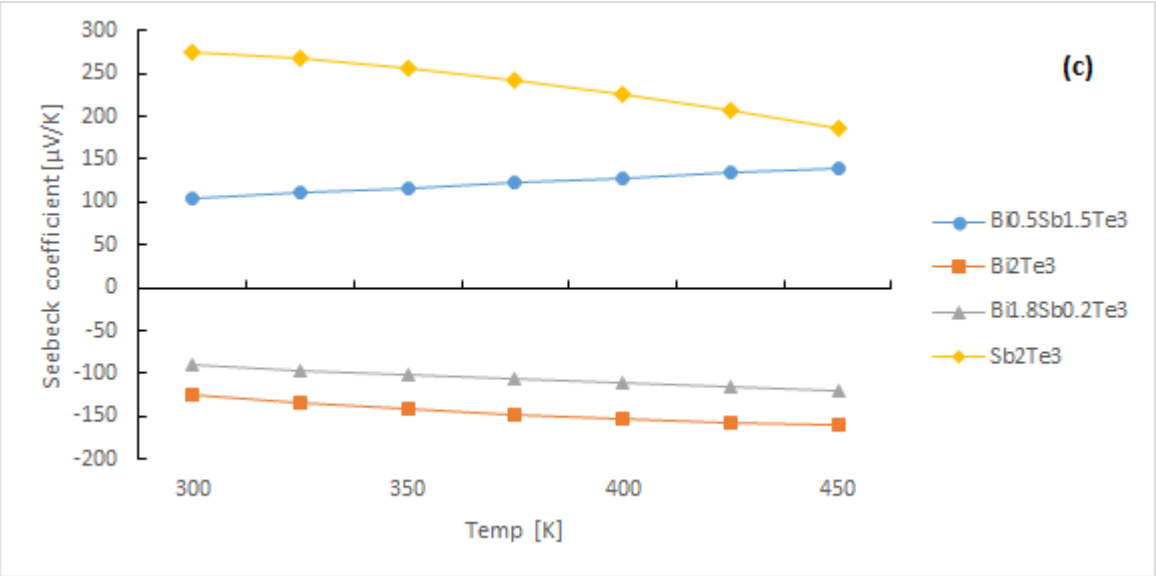
(c)
Seebeck coefficient [µV/K]
300
250
200
150
100
50
0
-50
-100
-150
-200
300
350
400
450
Temp [K]
Bi0.5Sb1.5Te3
Bi2Te3
Bi1.8Sb0.2Te3
Sb2Te3

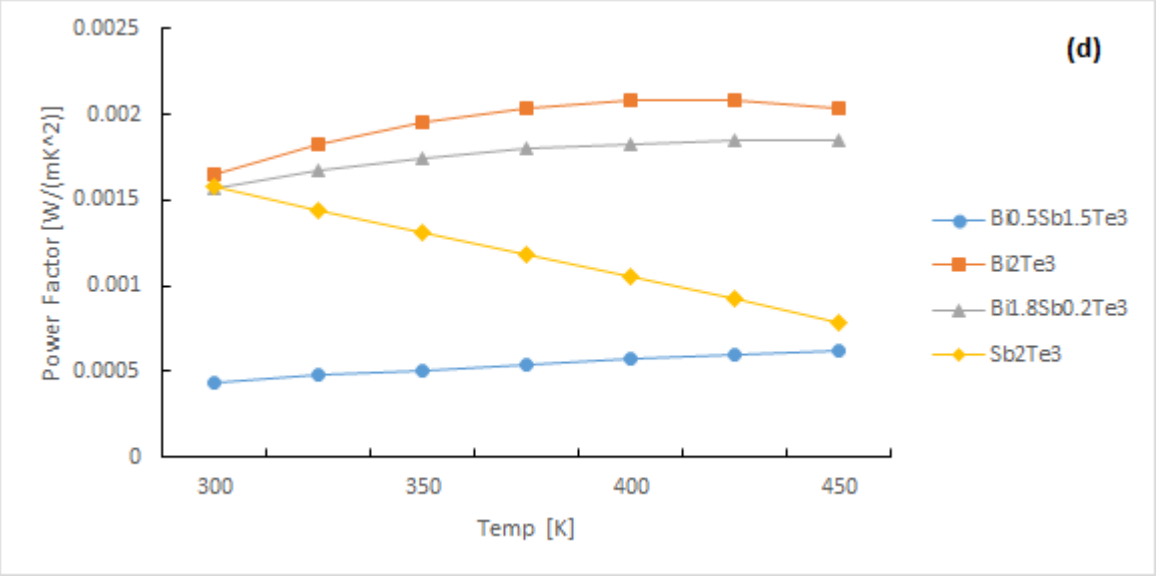
(d)
Power Factor [W/(mK^2)]
0.0025
0.002
0.0015
0.001
0.0005
0
300
350
400
450
Temp [K]
Bi0.5Sb1.5Te3
Bi2Te3
Bi1.8Sb0.2Te3
Sb2Te3

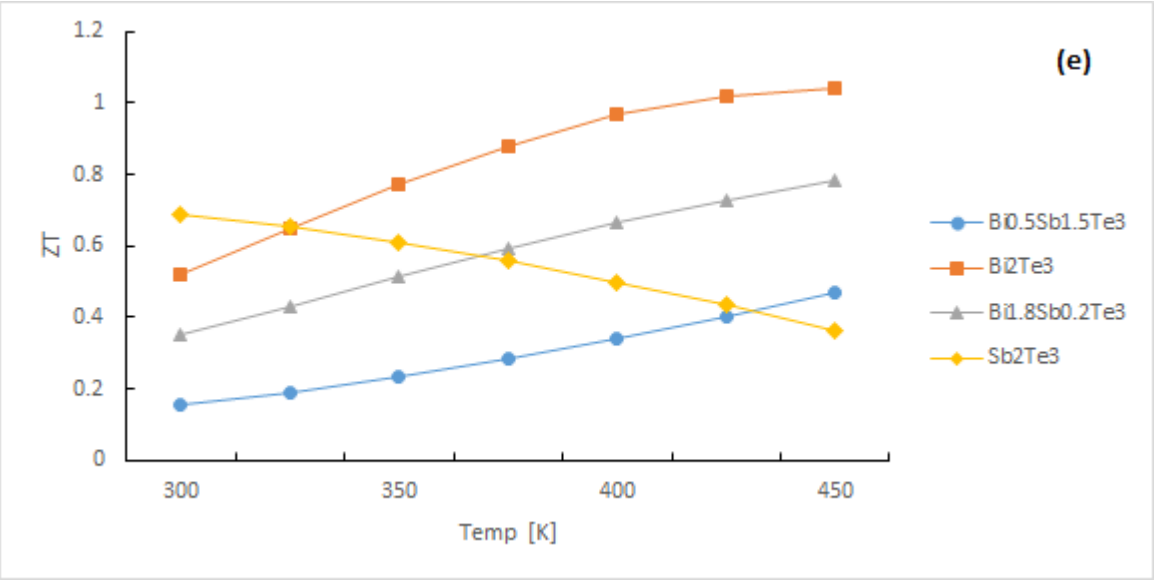

Figure 14. The temperature dependent transport properties of the synthesized $Bi_{2-x}Sb_xTe_3$ samples, (a) electrical conductivity, (b) thermal conductivity, (c) Seebeck coefficient, (d) Power factor, (e) figure of merit ZT.

When comparing the graphs from figure 14 (e), the most surprising aspect is the relatively low ZT of $Bi_{0.5}Sb_{1.5}Te_3$, and for that part, most of the thermal properties as well. When compared to the results of the other samples and the literature the RT ZT of 0.153 is somewhat low [8, 12]. Many sources claim the $Bi_{0.5}Sb_{1.5}Te_3$ composition to be the best performing composition of the entire $Bi_{2-x}Sb_xTe_3$ system[10, 17, 18]. To understand why the ZT is low one most look at the individual coefficients, such as the Seebeck coefficient seen in (c) and the electrician and thermal conductivity (a) and (b) respectively. When comparing these variables to the literature [12, 36, 37] it can be seen that the factors which contribute most negatively to the ZT value are the low Seebeck coefficient and electrical conductivity which together gives a low power factor which can be observed from (d). TE transport properties are sensitive when it comes to the composition and the crystal structure of the material. It's also worth to note the relative density of the $Bi_{0.5}Sb_{1.5}Te_3$ pellets going up to 80%, which also can affect the material transport properties. As was seen from the XRD plots of the pellets, the intensity changed from the SPS process but the position of the peaks are the same, which could be an explanation for some of these factors. An SPS compression going awry would affect the material properties, and it could be suggested to optimize the SPS process for each composition as the same process might now be ideal for all of the different compositions and lead to some samples having higher or lower densities. SPS can be hard to get completely right as it's hard to get proper consistency of the SPS parameters, and usually trials are needed to improve on the parameters of the sintering. To achieve high consistency in the compression method, is therefore of high importance and finding techniques which help in this should be a focus for future research.

When comparing the transport properties of Sb_2Te_3 to the literature the ZT 0.69 at room temperature is comparable to the highest values from the literature or above [8, 10]. The ZT value 0.4 at 448 K is comparable to some stat-of-the-art devices. Most notable the Seebeck

coefficient is relatively high with a range of 300-200 μV/K for the 300-450K range, which is higher than many other reported Seebeck values. The thermal and electrical conductivities are in comparable levels with earlier reports[8–11, 27].

The Bi_2Te_3 with the ZT value of 1.04 at 448K is on par with the state-of-the-art values from the literature where the highest values are 1.0 or slightly above. The transport properties are as well comparable to some of the highest reported values, with a Seebeck value of -124 at RT and the max value of -160 μV/K and a thermal conductivity of 0.875 W/mK being high values. The σ with 1000 S/cm is a high value, but not as high as some other reported values such as 1300 S/cm. [8, 11, 21, 27, 31, 35]

The $Bi_{1.8}Sb_{0.2}Te_3$ sample had the second highest ZT of the samples which is good for the p-n transition aspect. The $Bi_{0.5}Sb_{1.5}Te_3$ sample had not as high ZT in comparison. Potentially these two materials can be used together at 375 K, or at 450 K in a TE device and have a relative high efficiency with low thermal expansion.

Comparisons of the experimental values and ZT values from the literature can be seen in Table 2 and 3, at 300 K and 450 K respectively. The literature values chosen were amongst the best values found for their respective compositions, where the processing of the materials have shown a great diversity. Generally, the experimental values can be considered to be functional and, in some cases, up to state-of-the-art level.

Table 2. ZT values at 300K of prepared n- and p- type nano-TE materials with relevant literature.

T: 300 K	Bi_2Te_3	$Bi_{1.8}Sb_{0.2}Te_3$	$Bi_{0.5}Sb_{1.5}Te_3$	Sb_2Te_3
Obtained ZT	0.52	0.35	0.15	0.69
LiteratureZT [8]	1.1	0.7	1.16	0.74

Table 3. ZT values at 450K of prepared n- and p- type nano-TE materials with relevant literature.

T: 450 K	Bi_2Te_3	$Bi_{1.8}Sb_{0.2}Te_3$	$Bi_{0.5}Sb_{1.5}Te_3$	Sb_2Te_3
Obtained ZT	1.04	0.78	0.47	0.37
Literature ZT	1.0 [38]	--	0.5 [12]	0.7 [10]

3.3 Future work

A MW synthesis process have been successfully developed and used for synthesis of nanostructured TE materials from the BiSbTe system. For future works it would be interesting to try the same method for other systems and TE materials to see if this synthesis technique can be applied to other materials than the ones tested in this thesis. Looking further into using TE devices with materials close to the p-n transition would be an interesting project as well as building a complete device with those same materials. To compare their efficiency to devices with regular compositions to see if the advantage of having a better thermal expansion outweigh any possible advantage of the other devices would be of interest. Specifying the SPS parameter for each composition could be multiple projects in its own right, to make sure that each composition can be optimized.

4. Conclusions

A MW-assisted method was developed and used to synthesize TE nanopowders based on the $Bi_{2-x}Sb_xTe_3$ system. The resulting powders had good homogeneity and high batch to batch reproducibility, and it was deemed that the method has good reproducibility. The materials were made with the transition between p- and n- type materials in mind, as to lower any asymmetric thermal expansion in the TE device configuration. Pellets were made using SPS and their thermoelectric properties showed n- to p- type transition when $x > 0.5$. Finally, the highest ZT value of 1.04 was obtained for n-type and 0.4 for p-type synthesized materials at 448 K. These results are comparable to state-of the art values for n- and p-type bulk Bi-Te materials. The ease of synthetic process makes it a feasible process to scale-up for developing materials in large quantities for niche device applications.

5. Acknowledgements

I want to finish by giving my most sincere gratitude to a number of people who have helped me throughout this project. Starting with my examiner Prof. Muhammet Toprak who have given handy advice and allowed for this project to be made. My supervisor Mr. Bejan Hamawandi deserves a lot of my thanks, for guiding and helping me at every step on the way. Dr. Sedat Ballikaya from Istanbul University analyzed our pellets and obtained the transport properties data, and as such have been of great importance and deserve my thanks for helping with this task. I want to thank Rabia Akan and Hazal Batili for helping with the lab work and advice during the lab work. I want to thank the whole department of Applied Physics and more specifically the BIOX group whose members have been supporting and been helpful during the thesis work.

6. References

[1] E. Angeli *et al.*, "Nanotechnology applications in medicine," *Tumori*, vol. 94, no. 2, pp. 206–215, 2008.

[2] H. Komastu and A. Ogasawara, "Applying Nanotechnology to Electronics-Recent Progress in Si-LSIs to Extend Nano-Scale-," *Sci. Technol. Trends*, vol. 16, pp. 36–45, 2005.

[3] L. Yang, Z. G. Chen, M. S. Dargusch, and J. Zou, "High Performance Thermoelectric Materials: Progress and Their Applications," *Adv. Energy Mater.*, vol. 8, no. 6, pp. 1–28, 2018.

[4] "Thermoelectric device." [Online]. Available: http://www.personal.reading.ac.uk/~qf906281/Research/thermoelectric materials.html. [Accessed: 22-Nov-2018].

[5] Francis J. DiSalvo, "Thermoelectric Cooling and Power Generation," *Sci. New Ser.*, vol. 285, no. 5428, pp. 703–706, 1999.

[6] A. Malek Khachatourian, F. Golestani-Fard, H. Sarpoolaky, C. Vogt, and M. S. Toprak, "Microwave assisted synthesis of monodispersed $Y_2O_3$and Y_2O_3:Eu^{3+} particles," *Ceram. Int.*, vol. 41, no. 2, pp. 2006–2014, 2015.

[7] A. Baykal, M. Kizilyalli, M. Toprak, and R. Kniep, "Hydrothermal and Microwave Synthesis of Boron Phosphate, BPO_4," *Turkish J. Chem.*, vol. 25, no. 4, pp. 425–432, 2001.

[8] R. J. Mehta *et al.*, "A new class of doped nanobulk high-figure-of-merit thermoelectrics by scalable bottom-up assembly," *Nat. Mater.*, vol. 11, no. 3, pp. 233–240, 2012.

[9] S. Singh *et al.*, "Graphene-Templated Synthesis of c-Axis Oriented Sb_2Te_3 Nanoplates by the Microwave-Assisted Solvothermal Method," *Chem. Mater.*, vol. 27, no. 7, pp. 2315–2321, 2015.

[10] G.-H. Dong, Y.-J. Zhu, and L.-D. Chen, "Microwave-assisted rapid synthesis of Sb_2Te_3 nanosheets and thermoelectric properties of bulk samples prepared by spark plasma sintering," *J. Mater. Chem.*, vol. 20, no. 10, p. 1976, 2010.

[11] R. J. Mehta, C. Karthik, B. Singh, R. Teki, T. Borca-Tasciuc, and G. Ramanath, "Seebeck tuning in chalcogenide nanoplate assemblies by nanoscale heterostructuring," *ACS Nano*, vol. 4, no. 9, pp. 5055–5060, 2010.

[12] D. Suh *et al.*, "Enhanced thermoelectric performance of $Bi_{0.5}Sb_{1.5}Te_3$-expanded graphene composites by simultaneous modulation of electronic and thermal carrier transport," *Nano Energy*, vol. 13, pp. 67–76, 2015.

[13] K. Vanmeensel *et al.*, "Microstructure and mechanical properties of spark plasma sintered ZrO_2-Al_2O_3-$TiC_{0.5}N_{0.5}$ nanocomposites," *Solid State Phenom.*, vol. 106, no. 10, pp. 153–160, 2005.

[14] I. Álvarez-Clemares, A. Borrell, S. Agouram, R. Torrecillas, and A. Fernández, "Microstructure and mechanical effects of spark plasma sintering in alumina monolithic ceramics," *Scr. Mater.*, vol. 68, no. 8, pp. 603–606, 2013.

[15] R. S. S. Maki, S. Mitani, and T. Mori, "Effect of spark plasma sintering (SPS) on the thermoelectric properties of magnesium ferrite," *Mater. Renew. Sustain. Energy*, vol. 6, no. 1, p. 2, 2017.

[16] W. Wunderlich, T. Mori, and O. Sologub, "SPS-sintered $NaTaO_3$-Fe_2O_3composite exhibits enhanced Seebeck coefficient and electric current," *Mater. Renew. Sustain. Energy*, vol. 3, no. 1, 2014.

[17] P. Roy, V. Pal, and T. Maiti, "Effect of Spark Plasma Sintering (SPS) on the thermoelectric properties of $SrTiO_3$:15 at% Nb," *Ceram. Int.*, vol. 43, no. 15, pp. 12809–12813, 2017.

[18] S. W. Finefrock *et al.*, "Structure and thermoelectric properties of spark plasma sintered ultrathin PbTe nanowires," *Nano Lett.*, vol. 14, no. 6, pp. 3466–3473, 2014.

[19] S. Jin *et al.*, "Enhanced thermoelectric performance of P-type $Bi_xSb_{2-x}Te_3$nanowires with pulsed laser assisted electrochemical deposition," *Extrem. Mech. Lett.*, vol. 9, pp. 386–396, 2016.

[20] J. Navrátil, Z. Starý, and T. Plecháček, "Thermoelectric properties of P-type antimony bismuth telluride alloys prepared by cold pressing," *Mater. Res. Bull.*, vol. 31, no. 12, pp. 1559–1566, 1996.

[21] S. Li *et al.*, "Fabrication of nanostructured thermoelectric bismuth telluride thick films by electrochemical deposition," *Chem. Mater.*, vol. 18, no. 16, pp. 3627–3633, 2006.

[22] M. T. Pettes, J. Kim, W. Wu, K. C. Bustillo, and L. Shi, "Thermoelectric transport in surface- and antimony-doped bismuth telluride nanoplates," *APL Mater.*, vol. 4, no. 10, pp. 1–10, 2016.

[23] J. Zhang *et al.*, "Band structure engineering in $(Bi_{1-x}Sb_x)_2Te_3$ ternary topological insulators," *Nat. Commun.*, vol. 2, p. 574, 2011.

[24] D. Kong *et al.*, "Ambipolar field effect in the ternary topological insulator $(Bi_xSb_{1-x})_2Te_3$by composition tuning," *Nat. Nanotechnol.*, vol. 6, no. 11, pp. 705–709, 2011.

[25] E. Muller, W. Heiliger, P. Reinshaus, and H. Submann, "Determination of the Thermal Band Gap from the Change of the SEEBECK-Coefficient at the pn-Transition in (Bi0.5Sb 0.5)2Te3," *Fifteenth Int. Conf. Thermoelectr. Proc. ICT '96*, no. 1 996, pp. 412–416, 1996.

[26] H. Scherrer, B. Lenoir, A. Dauscher, and E. Mines, "Thermoelectric materials of P and N type from the (Bi ,Sb,Te) phase diagram," in *Proceedings ICT2001. 20 International Conference on Thermoelectrics*, 2001, pp. 13–17.

[27] C. Zhang, Z. Peng, Z. Li, L. Yu, K. A. Khor, and Q. Xiong, "Controlled growth of

bismuth antimony telluride $Bi_xSb_{2-x}Te_3$ nanoplatelets and their bulk thermoelectric nanocomposites," *Nano Energy*, vol. 15, pp. 688–696, 2015.

[28] N. Gerovac, G. J. Snyder, and T. Caillat, "Thermoelectric Properties of n-type Polycrystalline BixSbz- , Tes Alloys," in *Proceedings ICT 2002*, 2002, pp. 31–34.

[29] H. Kim, J. Lee, T. Oh, and D. Hyun, "Comparison of the thermoelectric properties of $(Bi,Sb)_2Te_3$ alloys prepared by powder metallurgy with single crystals," pp. 125–128, 1998.

[30] M. Y. Tafti *et al.*, "Promising bulk nanostructured Cu_2Se thermoelectrics: Via high throughput and rapid chemical synthesis," *RSC Adv.*, vol. 6, no. 112, pp. 111457–111464, 2016.

[31] W. Liu *et al.*, "Studies on the Bi_2Te_3-Bi_2Se_3-Bi_2S_3 system for mid-temperature thermoelectric energy conversion," *Energy Environ. Sci.*, vol. 6, no. 2, pp. 552–560, 2013.

[32] A. Saci, J. L. Battaglia, A. Kusiak, R. Fallica, and M. Longo, "Thermal conductivity measurement of a Sb_2Te_3 phase change nanowire," *Appl. Phys. Lett.*, vol. 104, no. 26, 2014.

[33] S. Il Kim *et al.*, "Dense dislocation arrays embedded in grain boundaries for high-performance bulk thermoelectrics," *Science (80-.).*, vol. 348, no. 6230, pp. 109–114, 2015.

[34] S. Katsuyama, Y. Kusafuka, and T. Tanaka, "Synthesis of $Bi_{0.5}Sb_{1.5}Te_3$ Sintered Composite with Dispersed Ionic Liquid and Investigation of Thermoelectric Properties " *Japan Soc. Powder Powder Metall.*, vol. 63, pp. 3–7, 2017.

[35] M. Saleemi, M. S. Toprak, S. Li, M. Johnsson, and M. Muhammed, "Synthesis, processing, and thermoelectric properties of bulk nanostructured bismuth telluride (Bi $_2$Te $_3$)," *J. Mater. Chem.*, vol. 22, no. 2, pp. 725–730, 2012.

[36] R. Deng *et al.*, "Thermal conductivity in $Bi_{0.5}Sb_{1.5}Te_{3+x}$ and the role of dense Dislocation Arrays At Grain Boundaries," *Sci. Adv.*, no. June, pp. 1–9, 2018.

[37] Ö. Ceyda Yelgel and G. P. Srivastava, "Thermoelectric properties of p-type $(Bi_2Te_3)_x(Sb_2Te_3)_{1-x}$ single crystals doped with 3 wt. % Te," *J. Appl. Phys.*, vol. 113, no. 7, 2013.

[38] L. B. Kong, T. Li, H. H. Hng, F. Boey, T. Zhang, and S. Li, *Waste Energy Harvesting*. Springer-Verlag Berlin Heidelberg, 2014.

Appendix

Table 1. $Bi_{2-x}Sb_xTe_3$ compositions and mass required for synthesis of 1g of the material.

	Elemental Composition			
	nBi	nSb	nTe	FW $Bi_{2-x}Sb_xTe_3$
$Bi_{2-x}Sb_xTe_3$	0.5	1.5	3	669.89
$Bi_{2-x}Sb_xTe_3$	1.8	0.2	3	783.18
$Bi_{2-x}Sb_xTe_3$	2	0	3	800.6
$Bi_{2-x}Sb_xTe_3$	0	2	3	626.32

Table 2. Molecular weight of the TE elements needed for 1g of the material.

Weight fraction of elements			Weight	Weight of elements		
wt fraction	wt fraction	wt fraction	TOT WT	wt Bi	wt Sb	wt Te
X Bi	X Sb	X Te	(g)	(g)	(g)	(g)
0.156	0.272	0.571	1.000	0.16	0.27	0.57
0.459	0.047	0.494	1.000	0.46	0.05	0.49
0.522	0.000	0.478	1.000	0.52	0.00	0.48
0.000	0.388	0.611	1.000	0.00	0.39	0.61

Table 3. Molecular weight of precursors needed for 1g of the TE material.

Amounts of precursor needed		
$BiCl_3$ (g)	$SbCl_3$ (g)	Te (g)
0.235	0.511	0.571
0.692	0.088	0.494
0.788	0.000	0.478
0.000	0.728	0.611